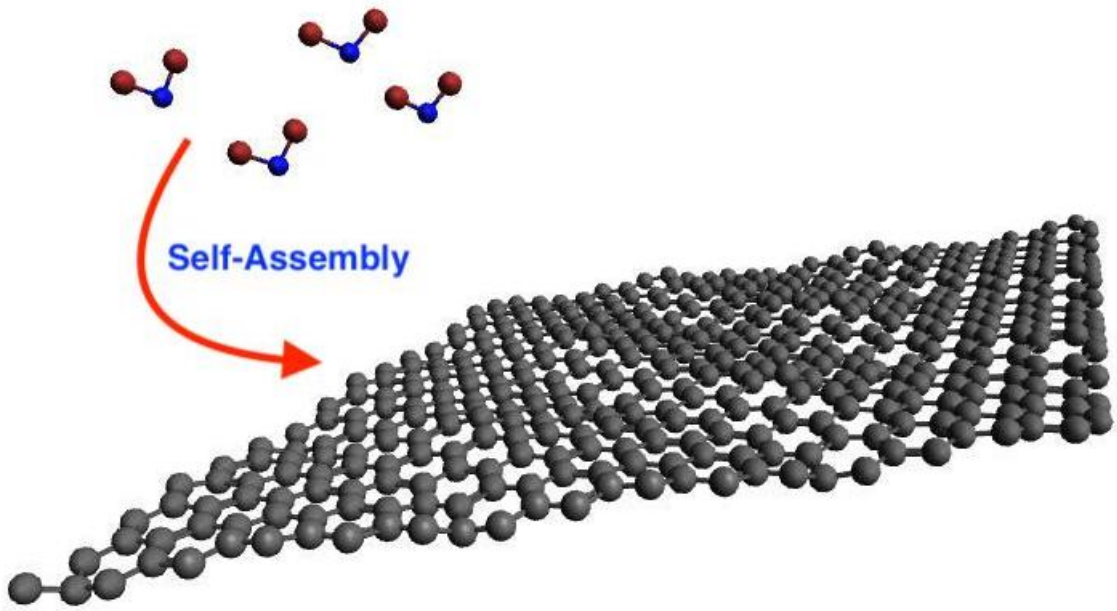



Figure 1: Graphical Abstract

# Ripples in Isotropically Compressed Graphene

Faris Abualnaja[a,b,c], Mariana Hildebrand[a,b], Nicholas M. Harrison[b]

[a]*Department of Physics, Imperial College London, Exhibition Road, SW7 2BP London, United Kingdom*
[b]*Department of Chemistry, Imperial College London, White City Campus, 80 Wood Lane, London W12 0BZ, United Kingdom*
[c]*Department of Electrical and Electronic Engineering, Imperial College London, Exhibition Road, SW7 2BP London, United Kingdom*

---

*Keywords:* Density Functional Perturbation Theory; Graphene; Isotropic Ripples; Elasticity; Molecular Self-Assembly

---

**Abstract**

*An isotropic compression of graphene is shown to induce a structural deformation on the basis of Density Functional Perturbation Theory. Static instabilities, indicated by imaginary frequency phonon modes, are induced in the high symmetry Γ - K (zigzag) and Γ - M (armchair) directions by an isotropic compressive strain of the graphene sheet. The wavelength of the unstable modes (ripples) is directly related to the magnitude of the strain and remarkably insensitive to the direction of propagation in the 2D lattice. These calculations further suggest that the formation energy of the ripple is isotropic for lower strains and becomes anisotropic for larger strains. This is a result of graphene's elastic property, which is dependent on direction and strain. Within the quasi-harmonic approximation this is combined with the observation that molecular adsorption energies depend strongly on curvature to suggest a strategy for generating ordered overlayers in order to tune the functional properties of graphene.*

---

*Email addresses:* f.abualnaja15@imperial.ac.uk (Faris Abualnaja), mariana.hildebrand13@imperial.ac.uk (Mariana Hildebrand), nicholas.harrison@imperial.ac.uk (Nicholas M. Harrison)

## 1. Introduction

Chemical functionalisation of graphene for real world applications has been a strong area of interest in academic and industrial research since the discovery of two-dimensional materials [1, 2, 3, 4, 5, 6, 7, 8, 9, 10, 11]. The addition of certain molecules on the surface of graphene can induce a change in its electronic characteristics, such as its band gap [1, 2, 12, 13, 14, 15, 16, 17, 18, 19] its electron mobility [1, 2, 3] and its electrical resistance [1, 2, 3, 8, 9, 10] . Moreover, any molecule that covalently binds onto the surface of graphene will undoubtedly alter its physical structure by disturbing its sp2 - backbone [12, 13, 14, 15, 16]. We have suggested in previous theoretical studies that such molecular patterns with long range order can tune the electronic band gap, magnetic coupling and transport properties of graphene [17, 18]. However, the patterning of molecular adsorption onto graphene has proved to be difficult, as grown structures tend to be stochastic in nature. A recent study, using Density Functional Theory (DFT) calculations, has shown that the curvature of graphene can significantly affect the binding energies of small (organic) molecules [19]. Depending on the nature of the bonding, chemi- or physisorbed molecules will bind to convex/concave regions in the rippled graphene [19, 20, 21, 22, 23, 24, 25, 26, 27, 28, 29, 30, 31]. In our previous work on the chemisorption of halogenated carbenes on graphene, we suggested a simple model that exploits the rippling behaviour of the graphene sheet in order to obtain, for that specific case, well-ordered and controllable molecular pattern formations [16]. In that instance, the rippling is generated spontaneously by adsorption induced strain. Moreover, recent theoretical studies on both strained graphene sheets and nanoribbons, have shown that graphene's electronic, magnetic, structural and mechanical properties can be tuned by varying the amount of compressive or tensile strain [32, 33, 34, 35]. In addition, graphene has shown to form ripples under strain [20, 21, 36, 37, 38]. For example, epitaxial graphene grown on a SiC (0001) substrate creates a lattice mismatch, straining the graphene sheet leading to a rippled structure [21, 38]. The strain on the graphene lattice and the resulting ripple formation arise from the lattice mismatch of the two materials [38]. Alternative substrates can be used to produce different strains to generate ripples of various wavelengths [39, 40]. For example, hexagonal Boron-

Nitride/Graphene heterostructures result in rippling as a strain-relieving mechanism, based on the lattice mismatch between the two materials [40]. Stretched polydimethylsiloxane (PDMS) films have also been suggested as substrates for graphene in order to induce different strains and thus ripples. The application of PDMS films with different pre-strains as substrates for graphene nanoribbons offers the possibility to generate ripples with varying morphology and periodicity [41]. In addition, a recent study compared the DFT calculation results of corrugated graphene on a SiC substrate to STM experiments [38]. It was found that a compressive strain of 5% gives a similar corrugation pattern to that obtained in experiments. Various studies have also shown that the elasticity of graphene varies with direction (see Figure 2) [42, 43, 44]. For example, previous studies have shown that armchair graphene nanoribbons (GNRs) have a higher Young's Modulus, tensile fracture stress and strain than zigzag GNRs of the same size [42, 43]. The increased stiffness of the graphene sheet in armchair direction would be expected to result in a lower out-of-plane (z-direction) distortion than that in the zigzag direction under the application of isotropic strain. The nonlinear in-plane elastic properties of graphene have also been studied by Wei *et al.* using DFT [44], where a Taylor expansion of graphene's elastic strain energy density, up to 5th order in the strain, is used to describe the thermodynamically favoured elastic response of graphene. This suggests a nonlinear behaviour at $\sim$5% strain and a noticeable anisotropy in elastic behaviour at > 5% strain. It is therefore expected that the elastic behaviour of graphene will significantly influence the ripple formation process.

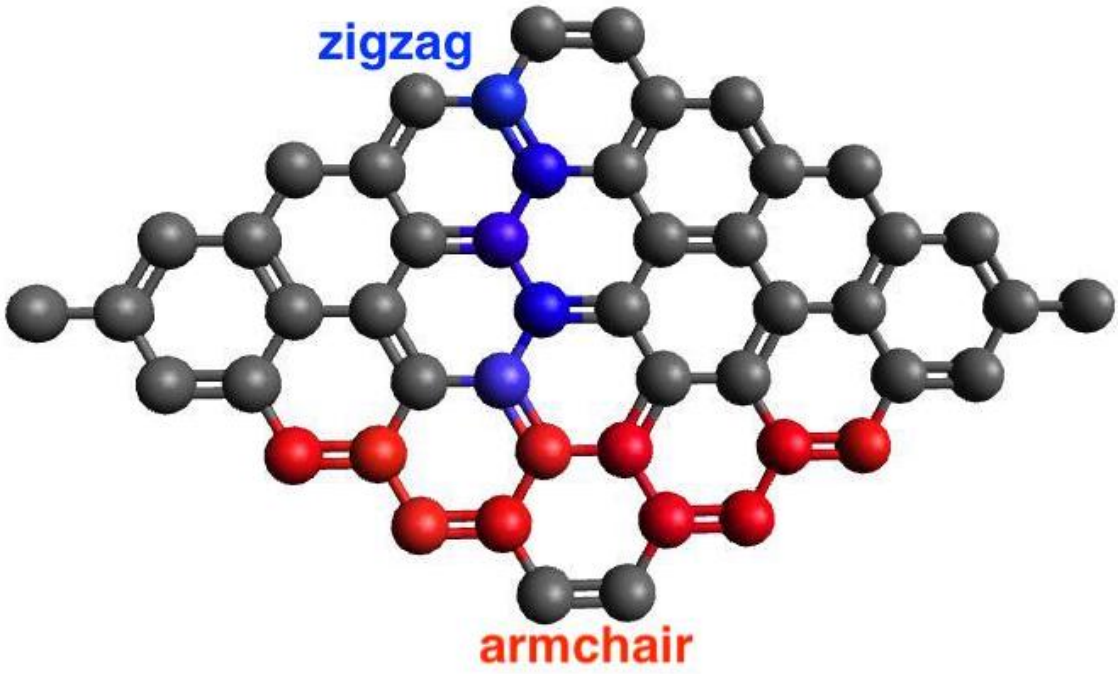



Figure 2: A graphene sheet indicating both the armchair (red) and zigzag (blue) directions.

In this work, we report on the structural characteristics and energetics of graphene under isotropic compression established using Density Functional Perturbation theory (DFPT) calculations. In the following sections we discuss the structural instabilities induced by strain, report on the energy of formation for various ripples and examine the influence of graphene's elasticity on the ripple formation.

## 2. Computational details

The Quantum Espresso (QE) program [45] has been used for the Density Functional Theory (DFT) and Density Functional Perturbation Theory (DFPT) calculations of the phonon frequencies reported here. A DFPT approach is favoured when calculating the phonon frequencies as it is less computationally expensive than alternative methods based on finite placements [46]. Exchange-Correlation effects are described within the Local Density Approximation (LDA) using the Perdew-Zunger (PZ) functional [47]. The crystalline orbitals are expanded in a plane-wave basis set

and the core electrons are replaced by a norm-conserving pseudopotential [45, 48]. A norm-conserving pseudopotential with an LDA functional is preferred when computing phonons in QE because it reduces the probability for producing an error when applying the Acoustic Sum Rule (ASR) [45]. The self consistent field was converged to a strict energy tolerance of $10^{-12}$ Ry for the phonon calculations. Moreover, the Brillouin zone (BZ) of the two - dimensional graphene lattice is sampled on a Monkhorst - Pack (MP) grid [49] of 3N x 3N in order to guarantee the correct sampling of the Dirac points, and to ensure an appropriate subdivision of the reciprocal lattice. It was found that an MP grid of 12 x 12 is sufficient for sampling the primitive cell, while an MP grid of 3 x 3 is sufficient for the supercells considered in this work. These calculations are then translated into real space using a Fourier transform approach, while applying the ASR [45, 46]. The Phonon Dispersion Curves (PDCs) are computed along the Γ - K - M - Γ high symmetry path using a mesh of 147 q-points. The initial geometry was a graphene sheet of lattice constant 2.46 Å [50] in a 3D periodic cell within which 2D periodic sheets are separated by a vacuum region of 10 Å which is sufficient to remove any interaction between periodic images. A Marzari-Vanderbilt cold smearing method [51] with a spread value of 8 x $10^{-3}$ Ry is applied. For self-consistency, the Davidson diagonalization procedure [52] with a mixing factor of 0.2 was used and self-consistency was considered to be achieved when the total energy per atom is less than of $10^{-4}$ Ry. Geometry relaxation was terminated when the largest inter-atomic force per atom was less than $10^{-3}$ Ry/Bohr between two consecutive iterations. Here, the sum over all inter-atomic forces is 0 ensuring a static structure. The optimised lattice constant is 2.46 Å, in excellent agreement with that observed in X-ray diffraction [50].

## 3. Results and Discussion

The computed phonon band structure for an unperturbed graphene sheet is presented in Figure 3 (solid black lines). The six phonon modes can be classified as optical (O) or acoustic (A). There are 3 acoustic modes (LA, TA, ZA) and 3N - 3 optical modes (LO, TO, ZO), where N = 2 is the number of atoms in the primitive cell. For each of these classes there is one in-plane longitudinal mode (LA, LO) and two transverse modes,

one in-plane (TA, TO) and one out-of-plane (ZA, ZO) [53]. Under zero strain all of the vibrational mode frequencies are positive indicating that the sheet is harmonically stable. Isotropic compressive strain is modelled by reducing the cell parameters under the constraint that the sheet retains the periodicity of the primitive cell.

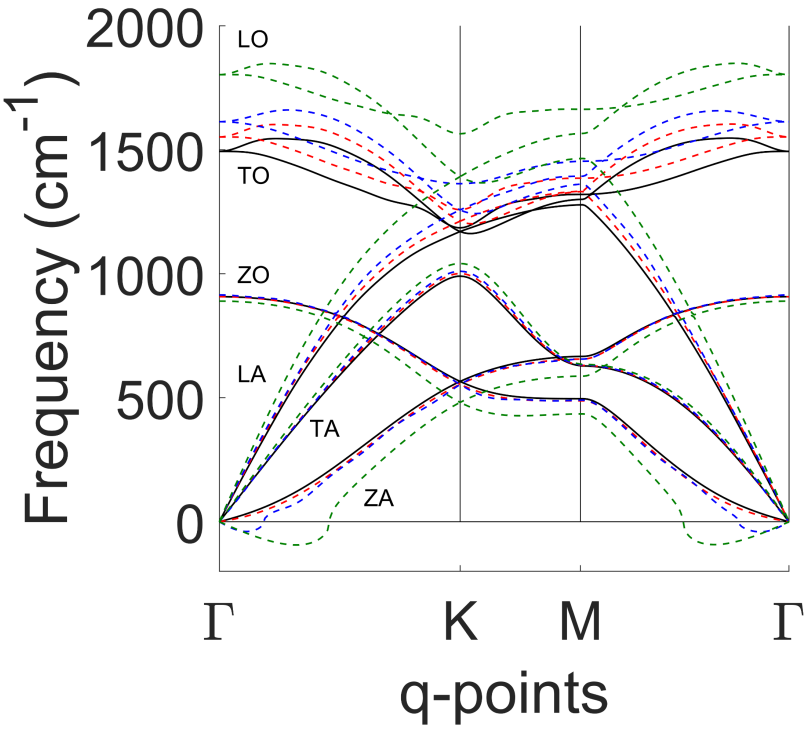



Figure 3: Phonon dispersion curve (PDC) of a graphene unit cell under 0% (black solid line), 1% (dashed red lines), 2% (dashed blue lines), and 5% (dashed green lines) isotropic compression. Strains greater than 1% induce negative frequencies for the ZA mode.

In Figure 3, the phonon band structures for 1%, 2% and 5% isotropic compressive strains are displayed as red, blue and green dashed curves respectively. The in-plane transverse and longitudinal mode frequencies generally increase as the C - C bonds are compressed. However, the out-of-plane transverse mode frequencies are significantly reduced. In certain q-point regions (Γ - K and Γ - M) the frequencies becomes negative (imaginary frequencies). This negative behaviour is apparent only for

the ZA mode. These out-of-plane distortions in the strained graphene sheet illustrate the unstable geometry and static ripple formations that may be modelled using the harmonic approximation. At 1% compressive strain (dashed red lines in Figure 3) the sheet is harmonically stable, while compressions greater than 2% (dashed blue and green lines in Figure 3) show sheet instabilities. These instabilities increase with greater strain as can be seen by the increased negativity at 5% compressive strain (dashed green lines in Figure 3). The imaginary (negative) frequencies are along the high symmetry Γ - K (zigzag) and Γ - M (armchair) directions, for both compressive strains. The q-vector corresponding to the most negative frequency ($\vec{q}_{min}$) for each strain provides an estimate of the wavevector of the distortion induced by the harmonic instability; the computed $|q_{min}|$ is a strong function of strain but a remarkably weak function of direction. This is further explored by plotting a higher resolution map of the calculated frequency of the ZA mode for the central region of the Brillouin zone (the region Γ - A - B - Γ, displayed for a strain of 5% in Figure 4). The fact that $|q_{min}|$ is, to a very good approximation, isotropic is immediately apparent.

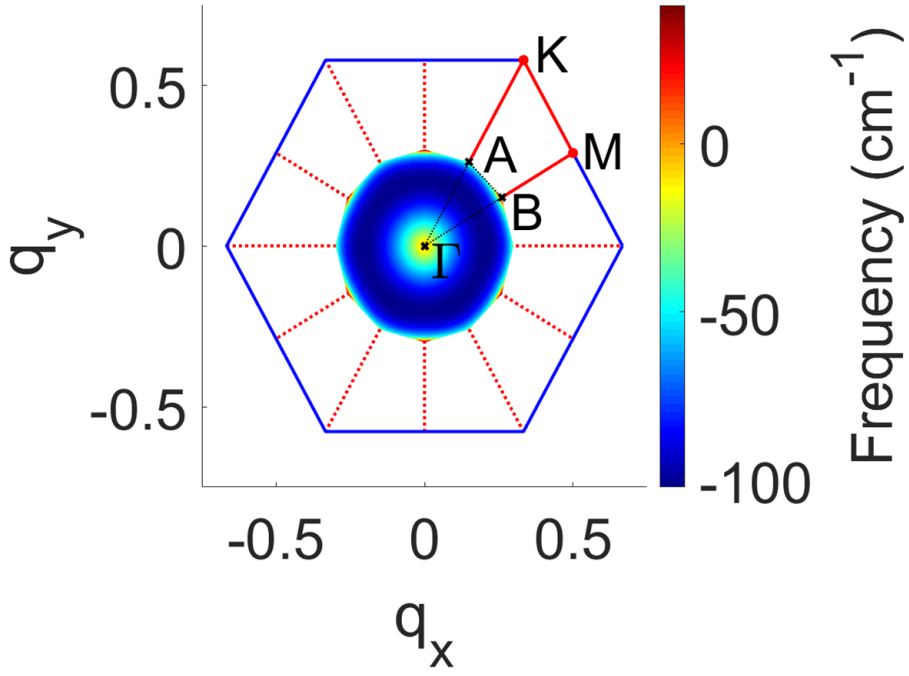



Figure 4: Phonon modes in the first Brillouin zones of a graphene sheet that is isotropically compressed by 5% showing negative, imaginary, frequencies within a smaller region defined by the path Γ - A - B - Γ.

At 2% strain, $|q_{min}|$ corresponds to a phonon wavelength that is along both the zigzag and armchair directions and is closely approximated by a ripple commensurate with a 10 x 10 supercell of the primitive graphene unit cell. Similarly, for 5% strain, $|q_{min}|$ corresponds to a phonon wavelength along the zigzag and armchair directions that are both closely approximated by a ripple commensurate with a 5 x 5 supercell of the primitive graphene unit cell. Using these commensurate supercells, the energy of phonon modes along the Γ - K (zigzag) and Γ - M (armchair) directions can be computed as a function of amplitude Δz. These energy profiles are presented in Figure 5. The minimum energy (or depth of the well) of the computed energy profiles (Figure 5) corresponds to the energetically most favoured Δz distortion (amplitude) and thus the preferred rippling configuration (or *stable ripple amplitude*).
At 2% strain, the armchair and zigzag modes have a similar stable ripple

amplitude of ∼0.19 Å (Figure 5a). At 5% strain, stable amplitudes are significantly different, ∼0.29 Å in the armchair direction and ∼0.63 Å in the zigzag direction. The distinctive difference in Δz distortion at 5% compressive strain (and the lack thereof at 2% compressive strain) can be explained by the simple notion that graphene's elasticity becomes anisotropic for both armchair and zigzag directions as a function of strain [42, 43, 44]. The anisotropic behaviour of the Γ - K (zigzag) and Γ - M (armchair) directions at 5% compressive strain (and the lack thereof at 2% compressive strain) furthermore suggests that the ripple formation process under isotropic compression is based on two competing effects, a) the energy gain through out-of-plane Δz distortions (*rippling*) and b) the elasticity of the sheet, which varies with direction and strain [42, 43, 44]. Based on the formalism of reference [44], we can therefore express the ripple formation energy as

$$E_{strain} - E_0 = E_{Ripple} = -\frac{1}{2}k(\Delta z)^2 + C_{IJ}\Omega_I\Omega_J \tag{1}$$

where $E_{strain}$ is the energy of the strained graphene sheet, $E_0$ is the energy of the unstrained, flat graphene sheet, $E_{Ripple}$ is the ripple formation energy, $k$ is related to the force constant of the ZA phonon mode and $\Delta z$ is the displacement along it, $C_{IJ}$ are the elastic constants (in Voigt notation) and $\Omega_I\Omega_J$ are the Lagrangian stresses. At small compressive strains, the difference in elastic constants for both armchair and zigzag directions is negligibly small, and the sheet shows isotropic behaviour, thus rippling unfavourably in any direction. At higher compressive strains (5% and more), the difference in elastic constants for both directions increases significantly, thus leading to anisotropic behaviour with the sheet preferably distorting in the zigzag direction.

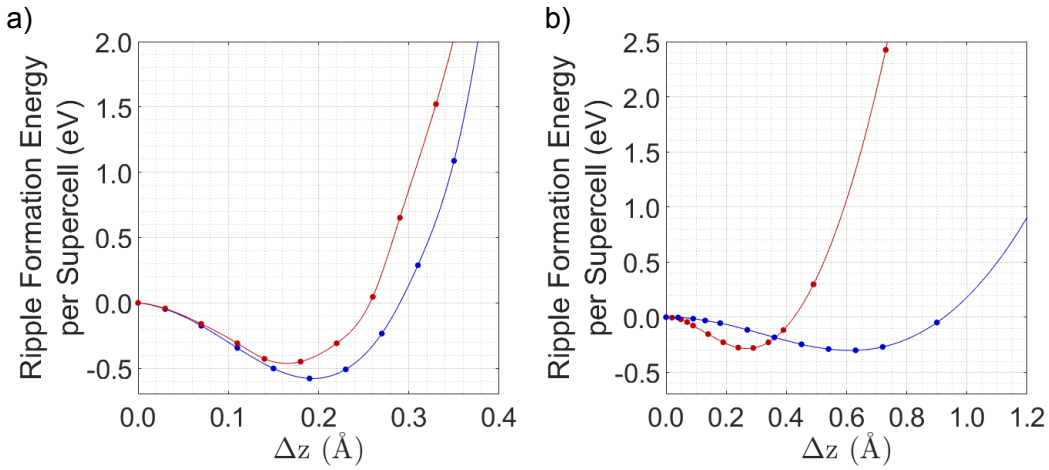



Figure 5: (a) Energy profiles of two phonon modes (armchair (red) and zigzag (blue) direction) under 2% compression at the minimum frequency of $\sim -24$ cm$^{-1}$ (minimum of dashed blue line in Figure 3, computed in a 10x10 supercell). (b) Energy profiles of two phonon modes (armchair (red) and zigzag (blue) direction) under 5% compression at the minimum frequency of $\sim -100$ cm$^{-1}$ (minimum of dashed green line in Figure 3, computed in a 5x5 supercell).

The harmonic distortion energy for forming ripples at the stable ripple amplitudes in both Γ - K (zigzag) and Γ - M (armchair) directions is comparable at both strains (Figure 5). At 2% strain the harmonic distortion energy for both modes (and thus directions) at the stable ripple amplitudes ($\sim$0.19 Å) is $\sim$ 0.5 eV per supercell (Figure 5a). 5% strain shows a harmonic distortion energy of $\sim$ 0.3 eV per supercell for both modes (and thus directions) at the stable ripple amplitudes ($\sim$0.29 Å and $\sim$0.63 Å, Figure 5b). However, overall, the zigzag direction is slightly lower in energy ($\sim$0.1 eV) for both strains and thus inconsiderably energetically favoured (blue curves in Figure 5a and 5b). The difference in energy between both Γ - K (zigzag) and Γ - M (armchair) directions is small enough that in a chemical environment, a combination of both ripple orientations is more likely for the compressive strains reported in this work. This has also shown to be true in our previous work on the chemisorption of halogenated carbenes, which suggests the likely formation of an eggbox-type (containing both armchair and zigzag ripple formations) structure [16]. However, in accordance with the results of reference [44], we expect

a more significant difference in ripple formation energy and thus an increased anisotropy between the Γ - K (zigzag) and Γ - M (armchair) directions at strains of > 5% [44].

## 4. Conclusions

In this work we have demonstrated a theoretical analysis of isotropically compressed graphene for the facilitation of chemical adsorption. Using Density Functional Perturbation Theory to examine a uniformly compressed graphene sheet, we find that the sheet is harmonically stable at 0 and 1% compressive strain. At 2 and 5% strain, two symmetric soft phonon modes along the Γ - K (zigzag) and Γ - M (armchair) directions are observed, suggesting a facile formation of periodic ripples in either direction. These lattice distortions have an associated ripple formation energy cost that is isotropic for smaller strains but becomes anisotropic for larger strains due to a direction and strain dependence of graphene's elasticity. The small energy difference between the armchair and zigzag directions for the strains reported here further suggests the formation of eggbox-type structures. These results will allow for controllable and well-defined molecular patterning by exploiting the curvature as induced by isotropic strain.

## 5. Acknowledgements

This research used resources of the National Energy Research Scientific Computing Center (NERSC), a U.S. Department of Energy Office of Science User Facility operated under contract no. DE-AC02- 05CH11231. The authors of this paper would also like to thank the High-Performance Computing service at Imperial College London for providing the required resources. Furthermore, we would like to thank Dr. Giuseppe Mallia and Zimen Makwana for valuable discussions in preparation of this paper.

## 6. Data Availability

The raw/processed data required to reproduce these findings cannot be shared at this time as the data also forms part of an ongoing study.

## References


[1] J. Warner, F. Schaeffel, A. Bachmatiuk, M. Ruemmeli, Graphene Fundamentals and Emergent Applications, Elsevier, (2013), p 336.

[2] K.D. Sattler, Handbook of Nanophysics: Functional Nanomaterials, CRC Press, (2010), p 7.

[3] S. Niyogi, E. Bekyarova, J. Hong, S. Khizroev,C. Berger, W. de Heer, R.C. Haddon, Covalent Chemistry for Graphene Electronics, J. Phys. Chem. Lett., 2 (2011), pp. 2487-2498.

[4] G. Hong, Q.-H. Wu, J. Ren, C. Wang, W. Zhang, S.-T. Lee, Recent Progress in Organic Molecule/Graphene Interfaces, Nano Today, 8 (2013), pp. 388-402.

[5] T. Sainsbury, M. Passarelli, M. Naftaly, S. Gnaniah, S.J. Spencer, A.J. Pollard, Covalent Carbene Functionalization of Graphene: Towards Chemical Band-Gap Manipulation, ACS Appl. Mater. Interfaces, 8 (2016), pp. 4870-4877.

[6] S.M. Clark, K-J. Jeon, J.-Y. Chen, C.-S. Yoo, Few-Layer Graphene Under High Pressure: Raman and X-ray Diffraction Studies, Solid State Commun., 154 (2013), pp. 15-18.

[7] S. Chun, Y. Kim, H. Jin, E. Choi, S.-B. Lee, W. Park, A Graphene Force Sensor with Pressure-Amplifying Structure, Carbon, 78 (2014), pp. 601-608.

[8] F. Schwierz, Graphene Transistors, Nat. Nanotechnol., 5 (2010), pp. 487-496.

[9] M.C. Lemme, T.J. Echtermeyer, M. Baus, H. Kurz, A Graphene Field-Effect Device Max, IEEE Electron Device Lett., 28 (2007), pp. 282-284.

[10] A. Pospischil, M. Humer, M. Furchi, D. Bachmann, R. Guider, T. Fromherz, T. Mueller, CMOS-Compatible Graphene Photodetector Covering all Optical Communication Bands, Nat. Photonics, 7 (2013), pp. 892-896.

[11] T. Georgiou, R. Jalil, B.D. Belle, L. Britnell, R.V. Gorbachev, S.V. Morozov, Y.-J. Kim, A. Gholinia, S.J. Haigh, O. Makarovsky, L. Eaves, L.A. Ponomarenko, A.K. Geim, K.S. Novoselov, A. Mishchenko, Vertical Field-Effect Transistor Based on Graphene- WS2 Heterostructures for Flexible and Transparent Electronics, Nat. Nanotechnol., 8 (2012), pp. 100-103.

[12] F. Karlicky, K.K.R. Datta, M. Otyepka, R. Zboril, Halogenated Graphenes: Rapidly Growing Family of Graphene Derivatives, ACS Nano, 7 (2013), pp. 6434-6464.

[13] M. Dubecky, E. Otyepkova, P. Lazar, F. Karlicky, M. Petr, K. Cepe, P. Banas, R. Zboril, M. Otyepka, Reactivity of Fluorographene: A Facile Way toward Graphene Derivatives, J. Phys. Chem. Lett., 6 (2015), pp. 1430-1434.

[14] W. Zan, Chemical Functionalization of Graphene by Carbene Cycloaddition: A Density Functional Theory Study, Appl. Surf. Sci., 311 (2014), pp. 377-383.

[15] I.K. Petrushenko, [2 + 1] Cycloaddition of Dichlorocarbene to Finite-Size Graphene Sheets : DFT Study, Monatsh. Chem., 145 (2014), pp. 891-896.

[16] M. Hildebrand, F. Abualnaja, Z. Makwana, N.M. Harrison, Strain Engineering of Adsorbate Self-Assembly on Graphene for Band Gap Tuning, J. Phys. Chem. C, 123 (2019), pp. 4475-4482.

[17] A.W. Robertson, B. Montanari, K. He, J. Kim, C.S. Allen, Y.A. Wu, J. Olivier, J. Neethling, N.M. Harrison, A.I.

Kirkland, J.H. Warner,. Dynamics of Single Fe Atoms in Graphene Vacancies, Nano Lett., 13 (2013), pp. 1468-1475.

[18] L. Pisani, B. Montanari, N.M. Harrison, A Defective Graphene Phase Predicted to be a Room Temperature Ferromagnetic Semiconductor, New J. Phys., 10 (2008), pp. 1-10.

[19] H. Pan, Waved Graphene: Unique Structure for the Adsorption of Small Molecules, Mater. Chem. Phys., 189 (2017), pp. 111-117.

[20] D.W. Boukhvalov, M.I. Katsnelson, Enhancement of Chemical Activity in Corrugated Graphene, J. Phys. Chem. C, 113 (2009), pp. 14176-14178.

[21] S. Goler, C. Coletti, V. Tozzini, V. Piazza, T. Mashoff, F. Beltram, V. Pellegrini, S. Heun, Influence of Graphene Curvature on Hydrogen Adsorption: Toward Hydrogen Storage Devices, J. Phys. Chem. C, 117 (2013), pp. 11506-11513.

[22] C.E Junkermeier, D. Solenov, T.L. Reinecke, Adsorption of NH2 on Graphene in the Presence of Defects and Adsorbates, J. Phys. Chem. C, 117 (2013), pp. 2793-2798.

[23] I. Fampiou, A. Ramasubramaniam, CO Adsorption on Defective Graphene-Supported Pt13 Nanoclusters, J. Phys. Chem. C, 117 (2013), pp. 19927-19933.

[24] S. Gotovac, H. Honda, Y. Hattori, K. Takahashi, H. Kanoh, K. Kaneko Effect of Nanoscale Curvature of Single-Walled Carbon Nanotubes on Adsorption of Polycyclic Aromatic Hydrocarbons, Nano Lett., 7 (2007), pp. 583-587.

[25] P. Zhang, X. Hou, J. Mi, Y. He, L. Lin, Q. Jiang, M. Dong, From Two-Dimension to One- Dimension: the Curvature Effect of Silicon-Doped Graphene and Carbon

Nanotubes for Oxygen Reduction Reaction, Phys. Chem. Chem. Phys., 16 (2014), p. 17479.

[26] S. Park, D. Srivastava, K. Cho, Generalized Chemical Reactivity of Curved Surfaces: Carbon Nanotubes, Nano Lett. , 3 (2003), pp. 1273-1277.

[27] V.S. Prudkovskiy, K.P. Katin, M.M. Maslov, P. Puech, R. Yakimova, G. Deligeorgis, Efficient cleaning of graphene from residual lithographic polymers by ozone treatment, Carbon, 109 (2016), pp. 221-226.

[28] G.Reza Yazdi, F. Akhtar, I.G. Ivanov, S. Schmidt, I. Shtepliuk, A. Zakharov, T. Iakimov, R. Yakimova, Effect of epitaxial graphene morphology on adsorption of ambient species, Applied Surface Science, 486 (2019), pp. 239-248.

[29] R. Balog, B. Jorgensen, J. Wells, E. Laegsgard, P. Hofmann, F. Besenbacher, L. Hornekaer, Atomic Hydrogen Adsorbate Structures on Graphene, JACS, 131 (2009), pp. 8744-8745.

[30] D.C. Elias, R.R. Nair, T.M.G. Mohiuddin, S. . Morozov, P. Blake, M.P. Halsall, A.C. Ferrari, D. . Boukhvalov, M.I. Katsnelson, A.K. Geim, 3 K.S. Novoselov, Control of Graphene's Properties by Reversible Hydrogenation: Evidence for Graphane, SCIENCE, 323 (2009), pp. 610-613, DOI: 10.1126/science.1167130.

[31] M. Bonfanti, Sticking of Atomic Hydrogen on Graphene, J. Phys.: Condens. Matter, 30 (2018), pp. 1-33, DOI: 10.1088/1361-648X/aac89f.

[32] S. Prabhakar, R. Melnick, Ab-initio Calculations of Strain Induced Relaxed Shape Armchair Graphene Nanoribbon, Physica E: Low-dimensional Systems and Nanostructures, 114 (2019), p. 113648, DOI: https://doi.org/10.1016/j.physe.2019.113648.

[33] I.Y. Sahalianov, T.M. Radchenko, V.A. Tatarenko, G. Cuniberti, Y.I. Prylutskyy, Straintronics in graphene: Extra Large Electronic Band Gap Induced by Tensile and Shear Strains, J. Appl. Phys., 126 (2019), p. 054302, https://doi.org/10.1063/1.5095600.

[34] , S. Kaur, H. Sharma, V.K. Jindal, V. Bubanja, I. Mudahar, Graphene Nanoribbons under Axial Compressive and Point Tensile Stresses, Physica E: Low-dimensional Systems and Nanostructures, 111 (2019), pp. 1-12, https://doi.org/10.1016/j.physe.2019.02.018.

[35] M. Hammouri, I. Vasiliev, Ab-initio Study of the Electronic and Transport Properties of Waved Graphene Nanoribbons, Physica E, 89 (2017), pp. 170-176, DOI: https://doi.org/10.1016/j.physe.2017.02.019.

[36] A. Fasolino, J.H. Los, M. Katsnelson, Intrinsic Ripples in Graphene, Nat. Mater., 6 (2007), pp. 858-861.

[37] R.C. Thompson-Flagg, M.J.B. Moura, M. Marder, Rippling of Graphene, Europhys. Lett., 85 (2009), p. 46002.

[38] A. Rossi, S. Piccinin, V. Pellegrini, S. De Gironcoli, V. Tozzini Nano-Scale Corrugations in Graphene: A Density Functional Theory Study of Structure, Electronic Properties and Hydrogenation, J. Phys. Chem. C, 119 (2015), pp. 7900-7910.

[39] S. Deng, V. Berry, Wrinkled, Rippled and Crumpled Graphene: an Overview of FormationM-mechanism, Electronic Properties, and Applications, Materials Today, 19 (2016), pp.197-212, DOI: https://doi.org/10.1016/j.mattod.2015.10.002.

[40] D. Nandwana, E. Ertekin, Ripples, Strain, and Misfit Dislocations: Structure of Graphene-Boron Nitride Superlattice Interfaces, NanoLett, 15 (2015), pp. 1468-1475, DOI: https://doi.org/ 10.1021/nl505005t.

[41] Y. Wang, R. Yang,Z. Shi, L. Zhang, D. Shi, E. Wang, G. Zhang, Super-Elastic Graphene Ripples for Flexible Strain Sensors, ACS Nano, 5 (2011), pp. 3645-3650, DOI: 10.1021/nn103523t.

[42] G. Georgantzinos, G.I. Giannopoulos, D.E. Katsareas, P.A. Kakavas, N.K. Antifantis, Size- Dependent Non-Linear Mechanical Properties of Graphene Nanoribbons, Comp. Mat. Science, 2011, pp. 2057-2062.

[43] X. Quin, W. Yan,X. Guo, T. Gao, Effects of Area, Aspect Ratio and Orientation of Rectangular Nanohole on the Tensile Strength of Defective Graphene – a Molecular Dynamics Study, Rsc. Adv., 8 (2018), pp. 17034-17043.

[44] X. Wei, B. Fragneuad, C.A. Marianetti, J.W. Kyssar, Non-linear Elastic Behaviour of Graphene: Ab Initio Calculations to Continuum Description, Phys. Rev. B, 80 (2009), p. 205407.

[45] P. Giannozzi, S. Baroni, N. Bonini, QUANTUM ESPRESSO: A Modular and Open-Source Software Project for Quantum Simulations of Materials, J. Phys.: Condens. Matter, 21 (2009), pp. 395-502.

[46] S. Baroni, S. de Gironcoli, A. Dal Corso, P. Giannozzi, Phonons and Related Crystal Properties from Density-Functional Perturbation Theory, Rev. Mod. Phys., 73 (2001), pp. 515.

[47] Jonsson,E.O.;Lehtola,S.;Jonsson,H. Towards anOptimal Gradient-Dependent Energy Functional of the PZ-SIC Form, Procedia Comput. Sci. 2015, 51, 1858-1864.

[48] K.F. Garrity, J.W. Bennett, K,M. Rabe, D. Vanderbilt, D. Pseudopotentials for High- Throughput DFT Calculations, Comput. Mater. Sci., 81 (2014), pp. 446-452.

[49] H.J. Monkhorst, J.D. Pack, Special Points for Brillouin-Zone Integrations, Phys. Rev. B: Solid State, 13 (1976), 13, p. 5188.

[50] D. Gray, A. McCaughan, B. Mookerji, Crystal Structure of Graphite, Graphene and Silicon, Physics for Solid State Applications, (2009); pp 1-20.

[51] N. Marzari, D. Vanderbilt, A. De Vita, M.C. Payne, Thermal Contraction and Disordering of the Al(110) Surface. Phys. Rev. Lett., 82 (1999), pp. 3296-3299.

[52] F.X. Gadea, Large Matrix Diagonalization, Comparison of Various Algorithms and a New Proposal, Chem. Phys. Lett. , 227 (1994), pp. 201-210.

[53] N.W. Ashcroft, D.N. Mermin, Solid State Physics, CBS Publishing Asia LTD., (1976).